J Mater Sci (2011) 46:3314–3318
DOI 10.1007/s10853-010-5218-5

Direct synthesis and hydrogen storage behaviors of nanocrystalline Na_2LiAlH_6

Xiulin Fan · Xuezhang Xiao · Lixin Chen · Shouquan Li · Hongwei Ge · Qidong Wang

Received: 18 July 2010 / Accepted: 24 December 2010 / Published online: 6 January 2011

Abstract Nanocrystalline Na_2LiAlH_6 was directly synthesized by mechanical milling 2NaH/LiH/Al mixture with TiF_3 catalyst under hydrogen pressure of 3.0 MPa. The synthesized Na_2LiAlH_6 exhibits a dehydriding capacity of 3.09 wt% in the first cycle, which is higher than that of Na_3AlH_6. Because of the complexity of mass transfer, the rehydrogenation process of the dehydrided Na_2LiAlH_6 is more intricate than that of the dehydrided sodium alanate, causing the formation of Na_3AlH_6 and the reduction of rehydriding capacity in the following cycles. As temperature increases from 70 to 120 °C, hydrogen absorption kinetics is extremely enhanced. The dehydrided material can reabsorb 80% of the reversible hydrogen capacity within 5 min when the temperature is above 100 °C with an initial hydrogen pressure of 4 MPa. The scanning electron microscopy and energy dispersive X-ray spectroscopy show that the as-synthesized Na_2LiAlH_6 along with the catalyst form a much homogeneous composite with a spherical particle size of 200 nm–2 μm.

Introduction

Onboard hydrogen storage has been recognized as one of several scientific challenges in promoting the hydrogen fuel cell-powered vehicle. Several solid-state storage media have been proposed, for example Mg-based hydrides [1–4], metal organic frameworks [1, 5], amides/imides [6, 7], and complex aluminum hydrides [7–10]. As potential solid-state hydrogen storage materials, complex aluminum hydrides have offered good perspectives due to their high hydrogen content and relatively low decomposition temperatures, since it was found that some transition metal halides (such as $TiCl_3$ and $CeCl_3$) can considerably lower kinetic barriers for both hydriding and dehydriding [8, 11]. Of the light representative of complex aluminum hydrides, sodium alanate with Ti-based additives has been systematically studied [12–18].

Sodium alanate can give a theoretical reversible hydrogen storage capacity of 5.6 wt% through the following two steps:

$$3NaAlH_4 \rightleftharpoons Na_3AlH_6 + 2Al + 3H_2 \quad (1)$$

$$Na_3AlH_6 \rightleftharpoons 3NaH + Al + 1.5H_2. \quad (2)$$

Recent investigation showed that the transition of NaH/Al to Na_3AlH_6 was the main block during the rehydrogenation of the NaH/Al mixture to $NaAlH_4$ [19]. With the full understanding of the behaviors of this hydrogenation process, we may develop methods to further improve the kinetics of hydrogenation. Moreover, it is known that if some Na^+ is substituted by Li^+ in sodium alanate, the hydrogen storage capacity will be further improved [20]. So it is of importance to examine the preparation and hydrogen storage characteristics of the intermediate state such as Na_3AlH_6, $Na_xLi_{3-x}AlH_6$ $(0 < x < 3)$. Thus, we chose Na_2LiAlH_6 as a representative specimen, and investigated its preparation methods and hydrogen storage behaviors.

Earlier, Na_2LiAlH_6 was synthesized using wet chemical method at relatively high temperature under high hydrogen pressure (usually under 30 MPa H_2 at 160 °C), and required filtering, washing, and drying to get a purified product [8, 21]. The whole process is quite intricate. So, there is a need for a low temperature and pressure preparation method which can give high yield without

X. Fan · X. Xiao · L. Chen (✉) · S. Li · H. Ge · Q. Wang
Department of Materials Science and Engineering, Zhejiang University, Hangzhou 310027, People's Republic of China
e-mail: lxchen@zju.edu.cn

purification steps. Recently, preparation of Na_2LiAlH_6 in the solid state by ball-milling of NaH–LiH–$NaAlH_4$, NaH–$LiAlH_4$ or $NaAlH_4$–$LiAlH_4$ mixtures has been described [22–28]. However, all of these methods involve alanates such as $NaAlH_4$ and $LiAlH_4$, which are also not easy to prepare.

Quite recently, Liu et al. [28] studied the mechanisms of the hydrogen desorption performance of the Ti fluoride catalyzed Na_2LiAlH_6, and stated that Ti and F play critical roles in the dehydrogenation/hydrogenation process of the Na_2LiAlH_6. Motivated by this, we performed a systematic investigation on the direct synthesis of Na_2LiAlH_6 by 2NaH/LiH/Al at the presence of TiF_3. In this study, we report that Na_2LiAlH_6 could be directly synthesized by dry mechanical milling 2NaH/LiH/Al with 4 mol% TiF_3 catalyst at ambient temperature. The prepared sample can reversibly absorb hydrogen at relatively low temperature under low hydrogen pressure. Besides this, it shows that the mass transfer is more complicated during the rehydrogenation process compared with that of dehydrided Na_3AlH_6.

Experimental

The starting materials of NaH powder (95%, <74 μm), Al powder (99%, <154 μm), LiH powder (98%), and TiF_3 powder were all purchased from Sigma-Aldrich Corporation. The powder mixture of NaH + LiH + Al + TiF_3 in a molar ratio of 2:1:1:0.04 were mechanically milled by Planetary mill at 300 rpm at ambient temperature. The milling vial and balls were made of stainless steel, and the weight ratio of balls to powder was 30:1. The milling was performed under 3 MPa hydrogen pressure. All the operations were performed inside a glove box under continuously purified argon atmosphere.

Hydrogen absorption/desorption behaviors were monitored with a Sievert's apparatus. The hydriding temperature range was 60–120 °C with 4 MPa. The dehydriding temperature range was 150–190 °C against 0.1 MPa. The samples were characterized by X-ray diffraction (XRD, ARL X'TRA, Thermo Electron Corp, CuK_α radiation) and Scanning electron microscopy (SEM, Hitachi S-4800) equipped with an energy dispersive X-ray spectroscopy analysis unit (EDS, EX350). The value of e-beam energy used in SEM measurements is 25 kV. Special caution had been taken to prevent the H_2O/O_2 contamination during the measurements.

Results and discussion

To investigate the phase transition during direct synthesis of Na_2LiAlH_6, the XRD patterns of the 2NaH/LiH/Al + 4 mol% TiF_3 mixture milled for a period ranging from 20 to 120 h and under 3 MPa hydrogen pressure are presented in Fig. 1. It is observed that only traces of Na_2LiAlH_6 show up at the first 20 h milling time, while NaH, LiH, and Al are still the dominating phases. As the milling time extends, the Na_2LiAlH_6 phase increases continuously. After 100–120 h milling time, the diffraction peaks for NaH become almost undetectable, signifying the reaction near completion. It should be noted that: LiH and Al can hardly be distinguished in patterns because of the similarity of their structures. In a comparative investigation, we failed to synthesize Na_2LiAlH_6 from the 2NaH/LiH/Al mixture without TiF_3 catalyst under an identical milling condition. We believe that upon doing with TiF_3 catalyst active Ti-species may be produced in the milling process and play a critical role in the in situ hydrogenation.

The SEM and EDS results of the as-synthesized Na_2LiAlH_6 sample prepared by ball milling for 120 h under 3 MPa hydrogen pressure are shown in Fig. 2. The sample has a wide range of size: some smaller particles have about 200 nm diameters, while some particles as large as 2 μm are also present. In higher magnification of SEM, we could see that most of these larger particles are formed by agglomeration of the small ones. Three different areas (labeled as A, B, and C) in Fig. 2a were characterized with EDS and the results show no difference (Fig. 2c). In addition, no phase contrast can be distinguished even in higher magnification (Fig. 2b). All of these suggest that after synthesis, the Ti and F containing species have been highly dispersed in the host hydride. It is hard to detect these species using the above XRD and SEM and EDS techniques, which is quite consistent with the former reported investigations [27–30]. By adding more TiF_3 (10 mol%) into Na_2LiAlH_6 systems, Nakamura et al. [30]

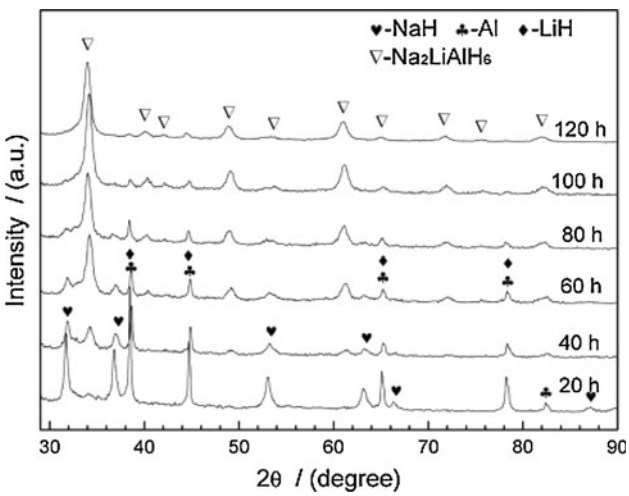

Fig. 1 XRD patterns of 2NaH/LiH/Al + 4 mol% TiF_3 milled for different milling time under 3 MPa hydrogen pressure

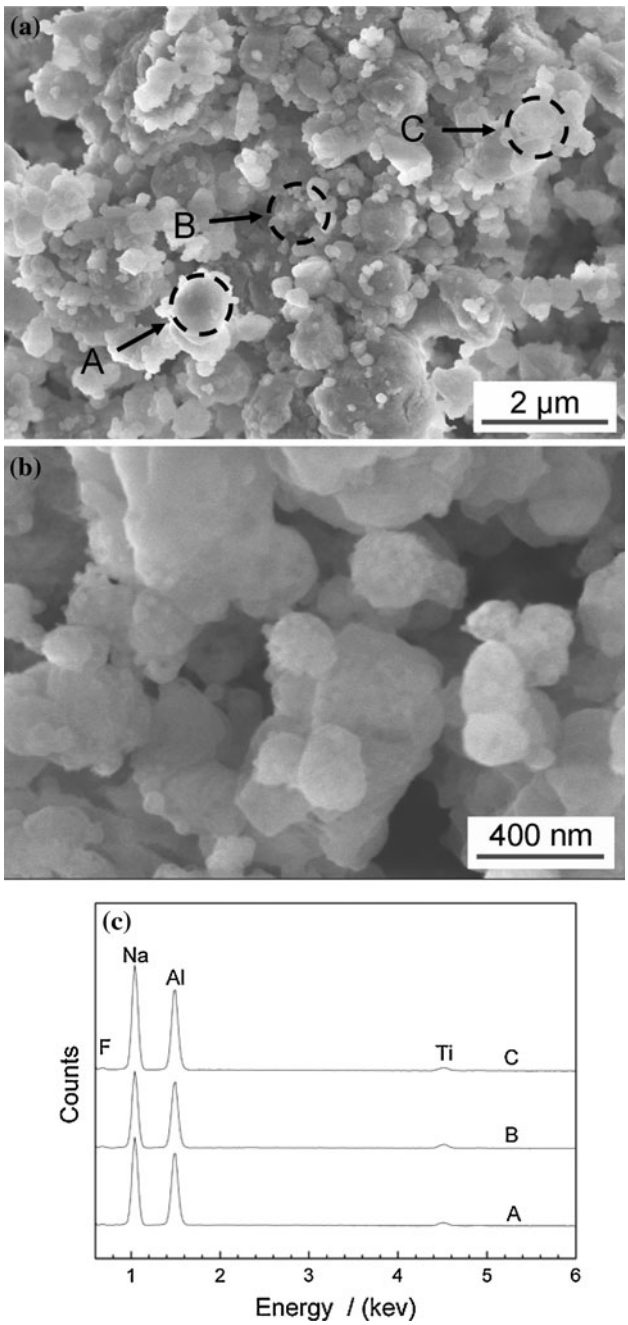

Fig. 2 Scanning electron micrographs and EDS results of 2NaH/LiH/Al + 4 mol% TiF_3 milled for 120 h under 3 MPa hydrogen pressure

still did not find any traces of Ti after ball milling. After several cycles, two types of Al–Ti phases were detected by synchrotron radiation powder XRD. Quite recently, using X-ray photoelectron spectroscopy analysis one of our authors [28] observed that Ti cations could be reduced to zero-valent Ti in the Na_2LiAlH_6 doped with 20 wt% Ti fluoride after ball milling. After several dehydrogenations at 260 °C, the formation of Ti–Al clusters was detected. However, due to the low concentration of TiF_3 in the system and the prolonged ball milling in this study, we

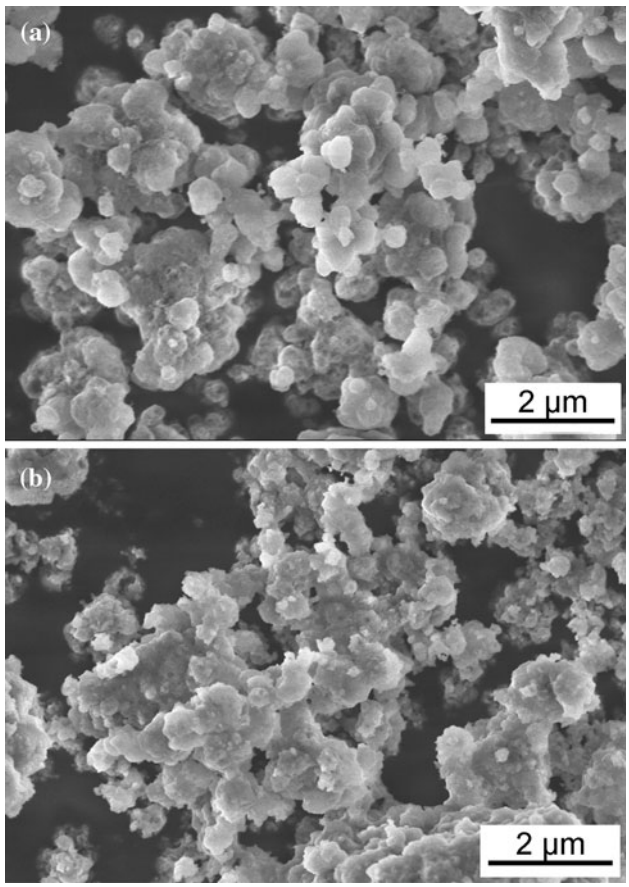

Fig. 3 Scanning electron micrographs of sample at different experimental stages: **a** after the second hydrogenation; **b** after the ninth dehydrogenation

could not detect the traces of effective catalyzing species. Yet, by comparing the doped material and the undoped mixture, we can basically reach the conclusion that Ti species, probably in the form of atomic Ti or Ti–Al clusters, account for the formation of Na_2LiAlH_6. Like in $NaAlH_4$ system, the Ti species may favor the mobility of Al-bearing species [31] and lowers the activation energy for the formation of Na_2LiAlH_6. However, for the undoped system, there is no such catalysis, and nothing more than milling could not give birth to Na_2LiAlH_6.

It is found that the hydrogenation–dehydrogenation cycles can alter the morphology of the particles significantly. Figure 3a shows electron micrograph taken after hydrogenation of the second cycle. It shows that after a hydrogenation–dehydrogenation cycle, the smallest particle size reaches about 500 nm, most of particles exhibit spherical form. The larger particles still remain about 2 μm. After ninth cycle, morphology of the particles changes greatly, presenting irregular form (Fig. 3b).

The dehydriding/rehydriding behaviors of the as-synthesized Na_2LiAlH_6 sample milled for 120 h have been investigated. At 150 °C, no hydrogen is released from the

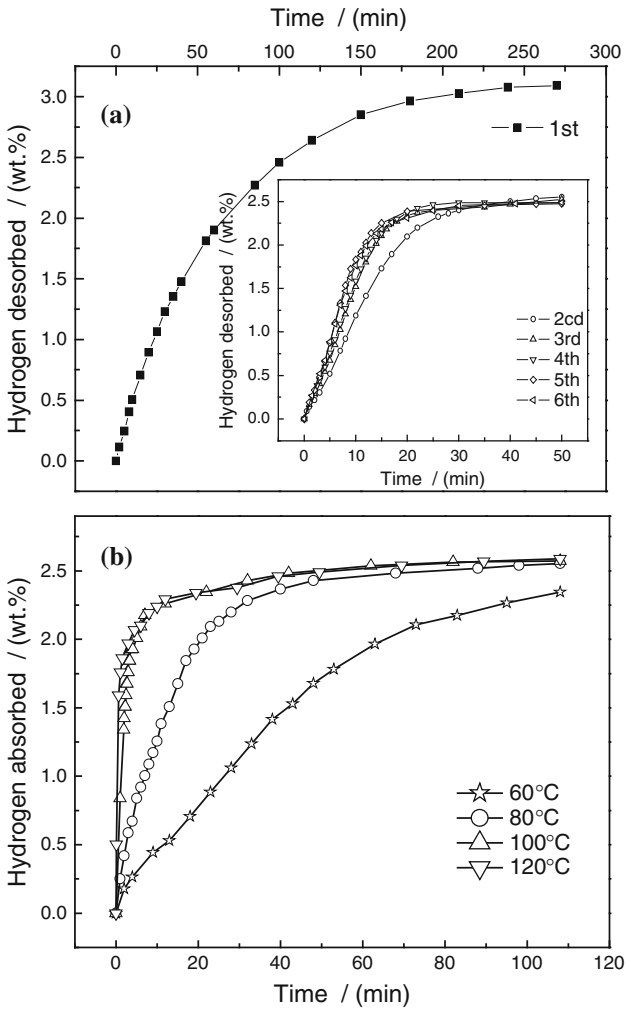

Fig. 4 Dehydriding/hydriding curves of the sample: **a** cycling dehydriding curves of the hydrided sample at 190 °C against 0.1 MPa pressure; **b** hydriding curves of the dehydrided sample at different temperature under 4 MPa hydrogen pressure

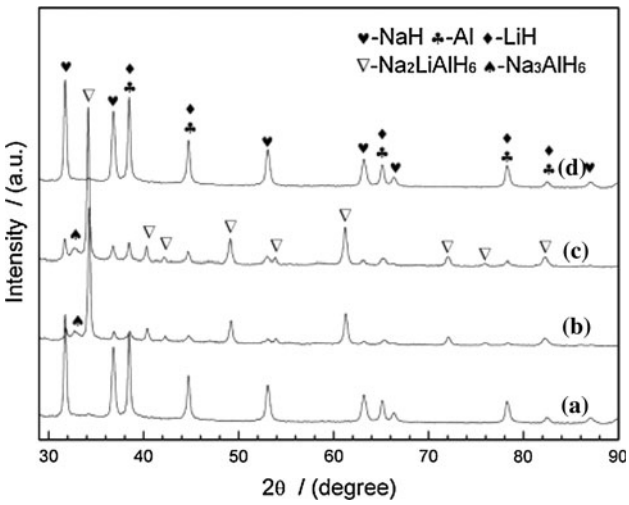

Fig. 5 XRD patterns of the sample containing 4 mol% TiF_3 at different experimental stages: (*a*) after dehydrogenation of the first cycle; (*b*) after hydrogenation of the second cycle; (*c*) after hydrogenation of the eighth cycle; (*d*) after dehydrogenation of the ninth cycle

as-synthesized Na_2LiAlH_6 against 0.1 MPa pressure, indicating that the hydrogen desorption plateau of Na_2LiAlH_6 is below 0.1 MPa at this temperature. At 190 °C, the dehydrogenation of the as-synthesized Na_2LiAlH_6 sample is achieved, and its cycling dehydriding curves are presented in Fig. 4a. The results show that the sample releases about 3.09 wt% H_2 at the first cycle within 4.5 h, which is lower than the theoretical reversible capacity of 3.5 wt%. However, if we take account of the alkali halide produced by the reaction between Ti halide and alkali hydride or alanate [32], the values fit well. The hydrogen desorption capacities in the following cycles show an obvious decrease compared with that in the first cycle. After that, the value remains almost unchanged in the following cycles. In the next four cycles, only about 0.1 wt% capacity was reduced. This phenomenon may be related to the complicated hydrogenation process, which causes the sample not fully restored and is discussed in the following paragraph. The dehydriding kinetics improve significantly in the first three cycles, which means that TiF_3-doped Na_2LiAlH_6 has to be activated by a cycling procedure to achieve an optimum kinetics. As rehydriding temperature increases from 60 to 120 °C, the hydriding rate is extremely enhanced due to the improvement of dynamic reactivity (Fig. 4b). In order to exclude the cycling effect on the rehydrogenation, the rehydriding data shown are all collected in the third cycle. It is found that the dehydrided sample can absorb 80% of the reversible hydrogen capacity at 100 °C within 5 min, and absorb 2.35 wt% hydrogen at 60 °C in 110 min.

To investigate the cause of the reduction of rehydriding capacity after the first cycle, the XRD patterns of the samples at different experimental stages are examined, presented in Fig. 5. For dehydrogenation, the sample was entailed on dehydriding at 190 °C for 5 h against 0.1 MPa. While for hydrogenation, the sample was subjected to hydriding at 120 °C for 5 h under an initial hydrogen pressure of 4 MPa. In the XRD patterns of the dehydrided samples, the diffraction peaks of Na_2LiAlH_6 have disappeared (shown in Fig. 5a, d). However, in the XRD patterns of the rehydrided samples, residual NaH, Al, and LiH can be observed (shown in Fig. 5b, c). These results suggest that the dehydrogenation reaction of the sample is fully completed, while its rehydrogenation reaction is not. Furthermore, some Na_3AlH_6 phase could also be observed in the rehydrided samples. One probable mechanism explaining the phenomenon is a mass transfer problem: during dehydrogenation, rather large metallic aluminum particles are formed, which has been evidenced by

Bogdanovic et al. [33] using NMR experiment and SEM investigations during sodium alanate desorption. When it comes to Na_2LiAlH_6, the mass transfer will become more complicated because more kinds of resultant will give birth during dehydrogenation. By fitting the kinetic data in the Ti fluoride-doped Na_2LiAlH_6, Liu et al. [28] analyzed the kinetic behaviors of the system with the Johanson–Methl–Avrami equation, and the results showed that the reaction was controlled by a diffusion mechanism. During the process of rehydrogenation, there will be not only Al mass diffusion, but also LiH mass transfer. The metallic aluminum particles would first react with neighboring LiH and NaH to form Na_2LiAlH_6 and then all of the particles would be coated by a layer of Na_2LiAlH_6, terminating the rehydrogenation reaction. At the presence of catalyst, Al atoms can be transferred via AlH_x vacancies which show a relatively high diffusion rate at moderate temperature [31, 34, 35], however, the mass transfer rate of LiH is much lower, thus causing the formation of some Na_3AlH_6. Although, at these conditions Na_2LiAlH_6 is more stable in thermodynamics [30].

Conclusions

In summary, direct synthesis of Na_2LiAlH_6 from 2NaH/LiH/Al was achieved by dry mechanical milling with 4 mol% TiF_3 catalyst under H_2 atmosphere at ambient temperature. The as-prepared Na_2LiAlH_6 has a wide distribution range of particle size from 200 nm to 2 μm. The synthesized Na_2LiAlH_6 exhibits a high dehydriding capacity of 3.09 wt% in the first cycle and a reversible hydrogen capacity of about 2.60 wt% in the following cycles. The complicated mass transfer during rehydriding process of the dehydrided sample induces the formation of some Na_3AlH_6 and the reduction of reversible hydrogen capacity in the following cycles.

Acknowledgements The authors wish to acknowledge the financial support of this research from the National Basic Research Program of China (Grant No. 2007CB209701), the National Natural Science Foundation of China (Grant No. 51001090, 50871099 and 50631020), the Program for New Century Excellent Talents in University (Grant No. NCET-07-0741), the University Doctoral Foundation of the Ministry of Education (Grant No. 20090101110050), and the China Postdoctoral Science Foundation (Grant No. 200902622).

References

1. Sahaym U, Norton MG (2008) J Mater Sci 43:5395. doi:10.1007/s10853-008-2749-0
2. Kwon SN, Mumm DR, Park HR, Song MY (2010) J Mater Sci 45:5164. doi:10.1007/s10853-010-4551-z
3. Grigorova E, Khristov M, Khrussanova M, Peshev P (2008) J Mater Sci 43:5336. doi:10.1007/s10853-008-2779-7
4. Song MY, Baek SH, Bobet JL, Kwon SN, Hong SH (2009) J Mater Sci 44:4827. doi:10.1007/s10853-009-3736-9
5. Rowsell JLC, Yaghi OM (2005) Angew Chem Int Ed 44:4670
6. Chen P, Xiong Z, Luo J, Lin J, Tan KL (2002) Nature 420:302
7. Graetz J (2008) Chem Soc Rev 38:73
8. Bogdanović B, Schwickardi M (1997) J Alloys Compd 253–254:1
9. Orimo S, Nakamori Y, Eliseo JR, Züttel A, Jensen CM (2007) Chem Rev 107:4111
10. Fan XL, Xiao XZ, Hou JC, Zhang Z, Liu YB, Wu Z, Chen CP, Wang QD, Chen LX (2009) J Mater Sci 44:4700. doi:10.1007/s10853-009-3726-y
11. Bogdanović B, Felderhoff M, Pommerin A, Schüth F, Spielkamp N (2006) Adv Mater 18:1198
12. Brinks HW, Jensen CM, Srinivasan SS, Hauback BC, Blanchard D, Murphy K (2004) J Alloys Compd 376:215
13. Jensen CM, Zidan R, Mariels N, Hee A, Hagen C (1999) Int J Hydrogen Energy 24:461
14. Fichtner M, Fuhr O, Kircher O, Rothe J (2003) Nanotechnology 14:778
15. Sandrock G, Gross K, Thomas G, Jensen C, Meeker D, Takara S (2002) J Alloys Compd 330–332:696
16. Lohstroh W, Fichtner M (2007) Phys Rev B 75:184106
17. Singh S, Eijt SWH, Huot J, Kockelmann WA, Wagemaker M, Mulder FM (2007) Acta Mater 55:5549
18. Onkawa M, Zhang S, Takeshita HT, Kuriyama N, Kiyobayashi T (2008) Int J Hydrogen Energy 33:718
19. Fang F, Zheng S, Chen G, Sang G, He B, Wei S, Sun D (2009) Acta Mater 57:1959
20. Genma R, Uchida HH, Okada N, Nishi Y (2003) J Alloys Compd 356–357:358
21. Claudy P, Bonnetot B, Bastide JP, Letoffe JM (1982) Mater Res Bull 17:1499
22. Huot J, Boily S, Güther V, Schulz R (1999) J Alloys Compd 283:304
23. Zaluski L, Zaluska A, Ström-Olsen JO (1999) J Alloys Compd 290:71
24. Ma XZ, Martinez-Franco E, Dornheim M, Klassen T, Bormann R (2005) J Alloys Compd 404–406:771
25. Brinks HW, Hauback BC, Jensen CM, Zidan R (2005) J Alloys Compd 392:27
26. Okada N, Genma R, Nishi Y, Uchida HH (2004) J Mater Sci 39:5503. doi:10.1023/B:JMSC.0000039274.80645.5d
27. Fossdal A, Brinks HW, Fonneløp JE, Hauback BC (2005) J Alloys Compd 397:135
28. Liu YF, Wang FH, Cao YH, Gao MX, Pan HG, Wang QD (2010) Energy Environ Sci 3:645
29. Kang XD, Wang P, Cheng HM (2007) Scripta Mater 56:361
30. Nakamura Y, Fossdal A, Brinks HW, Hauback BC (2006) J Alloys Compd 416:274
31. Ivancic TM, Hwang SJ, Bowman RC, Birkmire DS, Jensen CM, Udovic TJ, Conradi MS (2010) J Phys Chem Lett 1:2412
32. Fang F, Zhang J, Zhu J, Chen GR, Sun DL, He B, Wei Z, Wei SQ (2007) J Phys Chem C 111:3476
33. Bogdanovic B, Felderhoff M, Germann M, Härtel M, Pommerin A, Schüth F, Weidenthaler C, Zibrowius B (2003) J Alloys Compd 350:246
34. Walters RT, Scogin JH (2004) J Alloys Compd 379:135
35. Gunaydin H, Houk KN, Ozolins V (2008) Proc Natl Acad Sci USA 105:3673